CHAPTER THIRTEEN

Transport of a Caspase Inhibitor Across the Blood–Brain Barrier by Chitosan Nanoparticles

Müge Yemişci,[*] Yasemin Gürsoy-Özdemir,[*] Seçil Caban,[†] Ebru Bodur,[‡] Yılmaz Çapan,[†] *and* Turgay Dalkara[*]

Contents

* Institute of Neurological Sciences and Psychiatry and, Department of Neurology, Faculty of Medicine, Hacettepe University, Ankara, Turkey
† Department of Pharmaceutical Technology, Faculty of Pharmacy, Hacettepe University, Ankara, Turkey
‡ Department of Medical Biochemistry, Faculty of Medicine, Hacettepe University, Ankara, Turkey

Methods in Enzymology, Volume 508
ISSN 0076-6879, DOI: 10.1016/B978-0-12-391860-4.00013-6

Abstract

The current treatment of neurological and psychiatric diseases is far beyond being satisfactory. In addition to highly complex disease mechanisms, the blood–brain barrier (BBB) also remains as a challenge by limiting the delivery of the majority of currently available therapeutics to the central nervous system. Several approaches taking advantage of molecular and physicochemical characteristics of the BBB have been developed recently to improve drug delivery to the brain.

Here, we introduce a nanomedicine that can efficiently transport BBB-impermeable peptides to the brain. This nanomedicine is made of chitosan nanoparticles into which considerable amounts of a peptide can be incorporated. The nanoparticle surface is modified with polyethylene glycol to enhance the plasma residence time by preventing their capture by the reticuloendothelial system. Monoclonal antibodies against the transferrin receptor (TfR), which is highly expressed on the brain capillary endothelium, are conjugated to nanoparticles via biotin–streptavidin bonds. The activation of TfR by the nanoparticle–antibody complex induces transcytosis and thus delivers the loaded drug to the brain. Penetration of nanoparticles to the brain can be illustrated *in vivo* by intravital microscopy as well as *ex vivo* by fluorescence or electron microscopy. *N*-Benzyloxycarbonyl-Asp(OMe)-Glu(OMe)-Val-Asp(OMe)-fluoromethyl ketone (Z-DEVD-FMK)-loaded nanoparticles rapidly release their contents within brain parenchyma, inhibit ischemia-induced caspase-3 activity, and thereby provide neuroprotection.

1. Introduction

The blood–brain barrier (BBB) is formed by endothelial cells lining cerebral microvessels. They have no fenestrations, and the junctions between them are sealed by tight junction proteins to limit paracellular diffusion (Abbott *et al.*, 2006). Although this structure is fundamental for the normal function of the central nervous system (CNS), it also introduces a significant challenge in the treatment of brain diseases, as it severely restricts the transport of therapeutic drugs from blood to the brain. Only small molecules (<400 Da) that are lipid soluble pass the BBB in pharmacologically significant amounts (Pardridge, 2007). Essential nutrients like hexoses, amino acids, or peptides are transported by specific carriers or transporters located on the BBB (Begley, 1996; Pardridge, 2007). Similarly, only a small number of hydrophilic therapeutic agents can pass through the BBB by diffusion or facilitated transport, whereas some of these agents are pumped back into the circulation by efflux systems (Begley, 1996; Kreuter, 2001). Therefore, novel strategies are needed urgently to deliver therapeutics across BBB.

One of the recently developed strategies is the use of endogenous transporters localized on the brain capillary endothelium as drug carriers (Aktaş *et al.*, 2005; Kreuter, 2001). The transferrin receptor (TfR), especially the subtype-1, is highly expressed on the luminal side of brain capillary endothelium and could prompt receptor-mediated transcytosis across the BBB when activated (Jefferies *et al.*, 1984; Pardridge *et al.*, 1991). Although directly linking a therapeutic agent to the ligand of this receptor is a plausible strategy to deliver the agent to the brain, this approach can only deliver a limited amount of the drug, when the ratio of drug molecule to carrier protein is around one. On the other hand, it is possible to increase significantly this ratio by loading large amounts of therapeutic molecules into nanoparticles targeted to the carrier systems on the BBB. Indeed, conjugation of nanoparticles with monoclonal antibodies against the TfR1 (TfRMAb) has been shown to direct nanoparticles, together with their contents, into the CNS after systemic administration (Aktaş *et al.*, 2005).

Chitosan polymers are biocompatible and do not cause allergic reactions or immune rejection. Surface modifications, like adding hydrophilic coatings such as polyethylene glycol (PEG), increase the stability and half-life of chitosan nanoparticles in the systemic circulation by preventing their elimination via the reticuloendothelial system (Brigger *et al.*, 2002). Therefore, a larger dose of therapeutic agents can effectively be delivered across the BBB into the CNS with these nanoparticles targeted to the brain by bypassing systemic degradation. The enhanced brain delivery also reduces potential systemic side effects (Zensi *et al.*, 2009).

Caspase-3, among other caspases, is a potent mediator of apoptosis and plays an important role in neuronal death following global or focal cerebral ischemia (Chen *et al.*, 1998; Namura *et al.*, 1998). Caspase-3 is found as an inactive precursor and is cleaved into active subunits following an apoptotic signal (Chen *et al.*, 1998; Namura *et al.*, 1998). Importantly, administration of caspase-3 inhibitors or knocking out the caspase-3 gene leads to increased cell survival following cerebral ischemia, highlighting the critical role of caspases in ischemic injury (Hara *et al.*, 1997; Namura *et al.*, 1998; Schielke *et al.*, 1998). One of these inhibitors, *N*-benzyloxycarbonyl-Asp(OMe)-Glu(OMe)-Val-Asp(OMe)-fluoromethyl ketone (Z-DEVD-FMK), is a specific and irreversible inhibitor of caspase-3 and was shown to decrease infarct volume in experimental models of ischemia when given intracerebroventricularly (Hara *et al.*, 1997). Unfortunately, similar to several other caspase inhibitors, this peptide is unable to pass the BBB and cannot achieve therapeutic levels within the brain parenchyma after systemic administration.

Here, we introduce preparation of a nanomedicine that can transport Z-DEVD-FMK across the BBB and describe the methods evaluating its penetration to the brain and its effect on ischemia-induced caspase activity and stroke.

2. Preparation of Nanoparticles

Chitosan nanoparticles are prepared and loaded with Z-DEVD-FMK (Bachem, USA) and then targeted to the brain by conjugating them with an antibody against the TfR1 on the brain capillary endothelium, according to a previously developed method (Aktaş *et al.*, 2005; Karatas *et al.*, 2009). Chitosan polymers are first modified with PEG chains (PEGylation) to increase the plasma residence time of nanoparticles by inhibiting their capture and elimination via the reticuloendothelial system (Fig. 13.1). The PEGylated polymer (MeO-PEG-OCH_2CO_2H) is synthesized from commercially available MeO-PEG-OH (Sigma-Aldrich, St. Louis, MO) according to previously described procedures (Fernandez-Megia *et al.*, 2007; Royer and Anantharmaiah, 1979).

Briefly, the PEGylated and biotinylated chitosan (CS-PEG-BIO) is dissolved (1 mg/ml) in ultrapure water having an electrical resistance of 18 *M*Ω cm at 25 °C. Nanoparticles are formed from the polymer with ionic gelation by adding a tripolyphosphate (TPP; Sigma, St. Louis, MO) solution (0.84 mg/ml) as a cross-linker onto the chitosan solution in aqueous medium. Concentrations of the polymer and cross-linker solutions and the

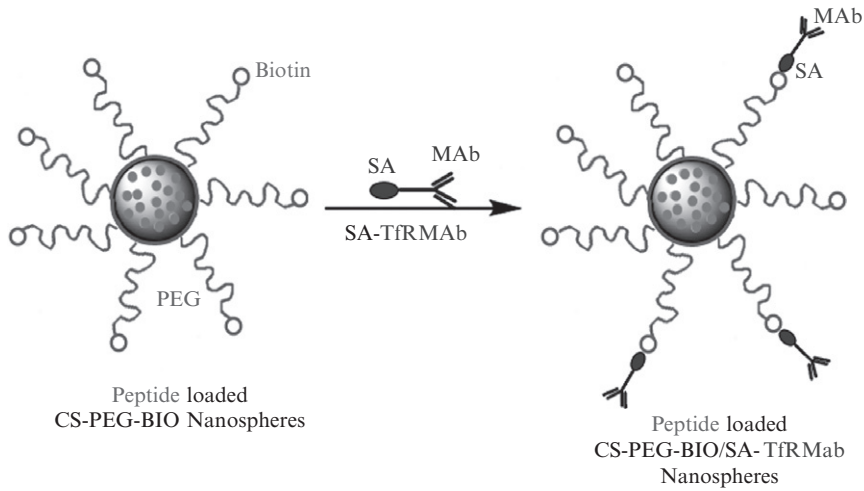

Figure 13.1 Schematic view of nanoparticles. Peptides such as caspase-3 inhibitor Z-DEVD-FMK or Nile red are loaded into chitosan nanoparticles. Their surface is then modified by adding poly(ethylene glycol) (PEG) chains and biotin (CS-PEG-BIO nanoparticles). Anti-mouse transferrin antibodies are conjugated with nanoparticles by means of biotin–streptavidin bonds (modified from Karatas *et al.*, 2009, with permission) (For interpretation of the references to color in this figure legend, the reader is referred to the Web version of this chapter.)

timing are kept constant in all batches to avoid undesirable aggregation or precipitation of nanoparticles as well as a highly variable particle size. The TPP solution is added drop wise onto the polymer solution while stirring. A fixed TPP dropping rate is used to obtain uniform batches. Z-DEVD-FMK (0.133 mg/ml) is incorporated into the polymer before the addition of TPP. The amount of Z-DEVD-FMK solution added is determined depending on the targeted loading concentration (e.g., 10.5 or 42 μl to obtain 50 or 188 ng/ml, respectively; see Section 4.2). The nanoparticle suspension is then centrifuged at 10,000 rpm (9277 × *g*) at 4 °C for 1 h and the supernatant is discarded.

2.1. Conjugation of streptavidin-monoclonal antibody complex with CS-PEG-BIO nanoparticles

Traut's Reagent (4 mg/ml) (2-immunothiolane, Pierce, Thermo Fisher Scientific Inc., Rockford, IL) solution is added into borate buffer and mixed with a Streptavidin (Sigma) solution (7 mg/250 μl water) in equal volumes for 90 min to obtain thiolate streptavidin. One hundred microliters of anti-TfR monoclonal antibody (TfRMAb; functional grade, purified, anti-mouse CD71, clone R17217, eBioscience, San Diego, CA) solution (1 mg/ml) is stirred with 5 μl of *m*-maleimidobenzoyl-*N*-hydroxysuccinimide (Sigma) solution (5 mg/ml in dimethylformamide) for 30 min at ambient conditions to transform some of the amino groups into maleimide groups. Equal volumes of the streptavidin solution and the antibody solution are then added into the CS-PEG-BIO nanoparticle suspension (500 μl). Finally, the mixture is vortexed for 1 min and kept at room temperature for 30 min.

2.2. Characterization of nanoparticles

Particle size and zeta potential measurements of the nanoparticles are performed in triplicate with standard protocols, as described before (Aktaş *et al.*, 2005; Karatas *et al.*, 2009). The drug amount adsorbed into the nanoparticles is calculated by the difference between the total amount of the peptide used and the amount of the nonencapsulated drug, which remains dissolved in the suspension.

For *in vitro* drug release studies, phosphate buffered saline (PBS, pH 7.4) is used as the medium in Eppendorf tubes in a water bath at 37 °C on a horizontal shaker. The supernatants are filtered through cellulose acetate filters before measuring the concentrations. Quantitation of Z-DEVD-FMK is achieved with HPLC (Agilent Technologies 1200 Series apparatus with HP CHEMSTATION software) and a cyano column (150 × 4.6 mm; particle size 5 μm; Clipeus, Higgins Analytical, Inc.). Mobile phase is a mixture of water:acetonitrile (80:20) containing 0.1% TFA. Twenty microliters of the

mobile phase is injected at a flow rate of 1 ml/min. Z-DEVD-FMK is detected at 215 nm wavelength (Aktaş *et al.*, 2005).

3. *In Vivo* Experiments with Nanoparticles Loaded with a Caspase Inhibitor

The penetration of nanoparticles into the brain *in vivo* can be monitored by using intravital fluorescence microscopy and can be verified by histopathologic evaluation of brain sections obtained from mice treated with nanoparticles (Karatas *et al.*, 2009). The *in vivo* neuroprotective effect of nanoparticles loaded with a caspase inhibitor is evaluated by using an experimental model of focal cerebral ischemia (Karatas *et al.*, 2009).

3.1. *In vivo* monitoring of nanoparticle penetration into the brain parenchyma by intravital fluorescent microscopy

Swiss albino mice are anesthetized with isoflurane during surgery and with urethane (750 mg/kg, intraperitoneal, followed by 500 mg/kg 30 min later) during the experiment. Physiologic parameters are closely monitored during the experiments: Body temperature is continuously measured by a rectal probe and kept at 37.0 ± 0.2 °C with a homeothermic blanket (Harvard Apparatus, Holliston, MA). Systolic blood pressure is monitored noninvasively by using a cuff and tail probe (NIBP controller; AD Instruments). Pulse rate and oxygen saturation are followed online by an oxymeter using a mini Y clip attached on the left lower extremity (V3304 Tabletop Pulse Oximeter; SurgiVet, Dublin, OH).

A cranial window of 5 × 5 mm is opened over the parietotemporal cortex, leaving the dura mater and cortex intact, blood pressure and oxygenation are maintained within normal limits in order to avoid cerebrovascular dysfunction. When drilling the cranial window, caution is taken for not heating the brain, hence, the cranium is frequently washed with saline. The cranium is firmly fixed to make sure that there is no head movement with the respiration of the animal. The window is sealed with dental acrylic and then filled with artificial cerebrospinal fluid (124 m*M* NaCl, 5 m*M* KCl, 1.25 m*M* NaH_2PO_4, 1.3 m*M* $MgSO_4$, 2.4 m*M* $CaCl_2$, 25 m*M* $NaHCO_3$, 10 m*M* glucose, pH 7.4) heated to 37 °C. The lightening conditions are kept constant for the recording of sequential fluorescence images throughout the experiment.

TfRMAb-conjugated or -unconjugated nanoparticles loaded with Nile red are administered intravenously via the tail vein of mice in order to assess the penetration of nanopheres into the brain parenchyma *in vivo*. Nile red is chosen as it emits intense fluorescence, is not biodegradable, can be reliably

detected by spectrophotometry, and can be efficiently loaded to nanoparticles (Gessner *et al.*, 2001). Fluorescent images are recorded under a Nikon Eclipse E600 microscope at 100 × magnification in dark by using a camera and imaging software (Nikon DXM1200 and NIS Elements Advanced Research v.2.32, Nikon) at baseline and after the injection of nanoparticles (1, 5, 10, 20, and 30 min after injection and then every 15 min for 3 h) using the same exposure time and gain settings. Images are saved in TIFF format to calculate the mean fluorescence intensity within the imaged area using the same imaging software.

The fluorescence emitted from TfRMAb-free nanoparticles, since they cannot pass the BBB, is as a reflection of Nile red fluorescence coming from nanoparticles in the brain circulation. On the other hand, the fluorescent signal emitted from TfRMAb-conjugated nanoparticles reflects the total pool of nanoparticles within the brain as well as circulation. Therefore, the difference between the fluorescent signals obtained in experiments performed with conjugated and unconjugated nanoparticles corresponds to the net signal coming from the nanoparticles penetrating the brain. Our experiments showed that the fluorescence from unconjugated nanoparticles peaked within 10 min of administration and gradually diminished over a period of 2 h, reflecting the elimination kinetics of circulating nanoparticles (Fig. 13.2). The fluorescence from TfRMAb-conjugated nanoparticles, however, continued to increase after the 10th minute of injection, and a significant signal was sustained during a 3-h follow up. The net difference between these curves suggests that nanoparticles functionalized with TfRMAb successfully penetrate into the brain tissue and this penetration starts as early as 10 min after systemic administration and reaches a peak within 75 min (Karatas *et al.*, 2009).

3.2. Determination of tissue Nile red concentration to evaluate nanoparticle distribution

UV spectrophotometry can be used to determine the tissue Nile red concentration in the brain, liver, and spleen. Tissues are homogenized (20%, w/v) in 25 m*M* HEPES (pH 7.4), 2 m*M* EDTA, 2 m*M* EGTA, 2 m*M* DTT, 5 m*M* $MgCl_2$, %0.1 Triton X-100 containing 10 μg/ml protease inhibitor cocktail and 3 ml of 1% phosphoric acid is added to 500 μl of homogenate to precipitate proteins followed by 3 ml of butanol to extract the lipid phase. The mixture is vortexed for 1 min at 2000 rpm and centrifuged at 2500 × *g* for 15 min. After this process, the extracted lipids as well as Nile red can be found in the upper butanol phase. Nile red in this media was found to have an absorbance peak at 549 nm through spectrophotometric analysis (Karatas *et al.*, 2009). No significant Nile red accumulation was detected in liver or spleen homogenates (Fig. 13.2). However, in brain homogenates of mice injected with TfRMAb-conjugated nanoparticles, there was a strong

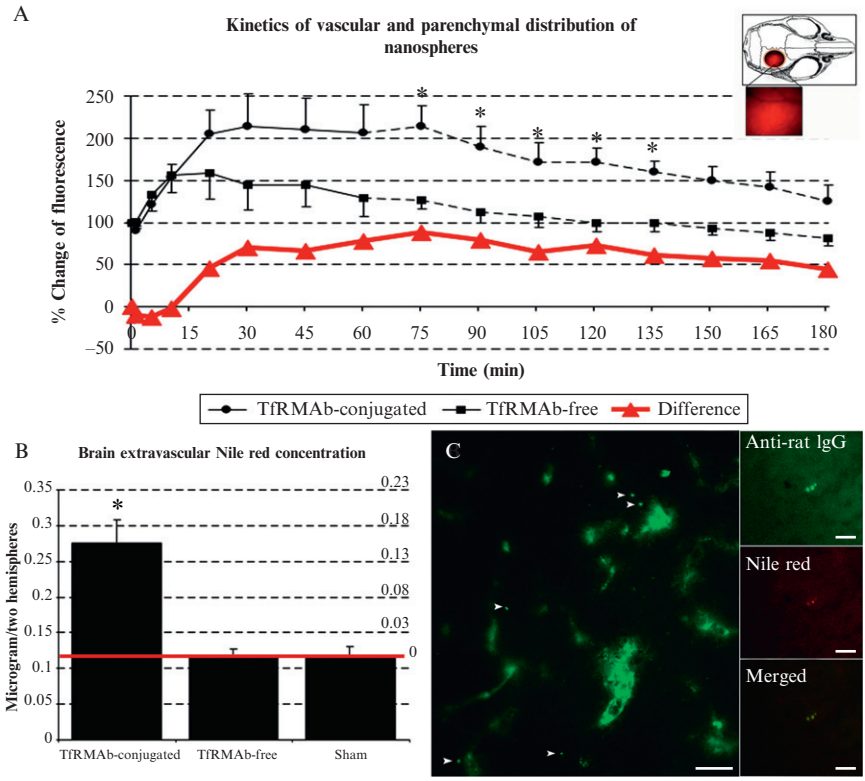

Figure 13.2 (A) Nanoparticles are rapidly transported to brain parenchyma after systemic administration. The graph illustrates the change in fluorescence recorded from the brain over the course of 3 h after injection of Nile red-loaded to TfRMAb-conjugated or -unconjugated nanoparticles. The difference between the two lines (red line) reflects the fluorescence coming from the nanoparticles within the parenchyma and illustrates the time course of nanoparticle penetrance to the brain. (B) Nile red concentration in brain postvascular tissue increased only when TfRMAb-conjugated nanoparticles were administered. The graph illustrates spectrophotometric measurements at 549 nm from brain homogenates obtained 1 h after injection of TfRMAb-conjugated or -unconjugated nanoparticles or from sham-operated mice. Only values above the horizontal red line, below which values correspond to the tissue background readings, were taken into consideration. (C) Penetration of the nanoparticles to the parenchyma was confirmed by fluorescent microscopy on brain sections obtained 1 h after injection. FITC-conjugated anti-rat IgG antibody (green) labeled the nanoparticles bearing TfRMAb, clearly demonstrating that the nanoparticles were dispersed within the extracellular space outside the vessel lumens. Vessels were visualized by nonspecific labeling obtained with a high concentration of the antibody. Some FITC-conjugated nanoparticles exhibited green as well as red fluorescence because they had not released within an hour all the Nile red that was loaded (right). A lower concentration of the antibody was used to stain these sections; hence, vessels were not labeled. Scale bars: (C) left panel, 15 μm; (C) right panels, 5 μm (reprinted from Karatas *et al.*, 2009, with permission).

spectrophotometric signal at 549 nm (Karatas *et al.*, 2009). These findings are consistent with the idea that TfRMAb conjugated to nanoparticles, being selective to the TfR type 1 on cerebral vasculature (Lee *et al.*, 2000), lead to preferential accumulation of nanoparticles in the brain.

3.3. Histological demonstration of nanoparticles within the brain parenchyma

The penetration of nanoparticles into the brain can also be demonstrated by using FITC-labeled nanoparticles and immunofluorescence microscopy. However, it is recommended that the examiner should familiarize himself with the appearance of nanoparticles first *in vitro* and then in sections prepared from mouse brains to which nanoparticles were directly injected. Nanoparticles appear as discrete fluorescent dots or as small aggregates in suspensions containing FITC-labeled nanoparticles (1 mg in 200 µl saline; Fig. 13.3). FITC-labeled nanoparticles (1 mg in 200 µl saline) are injected with a microsyringe into the right frontal cortex. Mice are immediately decapitated and the brains are kept at −80 °C until use. Frozen coronal sections of 20 µm thickness, passing through the injection site are then obtained and examined under fluorescence microscopy (Nikon Eclipse E600, λ_{ex} 450–490 nm). Nanoparticles are observed as fluorescent spherical particles, sometimes forming aggregates on brain sections, similar to their appearance in suspension (Fig. 13.3).

FITC-labeled (1 mg in 200 µl saline) TfRMAb-conjugated or -unconjugated nanoparticles are injected intravenously to mice via the tail vein. Mice are transcardially perfused with saline to flush the intravascular content, including the nanoparticles, and are then decapitated 1 and 2 h after injection. The sections are coverslipped with mounting medium containing Hoechst-33258 to counterstain the nuclei. The systemically administered TfRMAb-conjugated nanoparticles were distributed in both hemispheres (Fig. 13.3). The nanoparticles were localized in the brain parenchyma, outside the vascular lumen identified by the surrounding endothelial nuclei. However, no evidence for nanoparticle penetration into brain was observed in mice injected with nanoparticles not conjugated with TfRMAb (Aktaş *et al.*, 2005).

TfRMAb-conjugated nanoparticles loaded with Nile red can also be used to determine the passage of the nanoparticles through the BBB with help of their red fluorescence. At the end of the above described experiments performed with intravital fluorescence microscopy (Karatas *et al.*, 2009), mice are transcardially perfused with saline to flush all the intravascular content, including the nanoparticles loaded with Nile red. The brain, liver, and spleen are removed, immediately frozen, and kept at −80 °C until use. Fresh-frozen, 20 µm-thick coronal brain sections are cut, fixed with 96% ethanol for 10 min and washed with PBS. An antibody against the rat

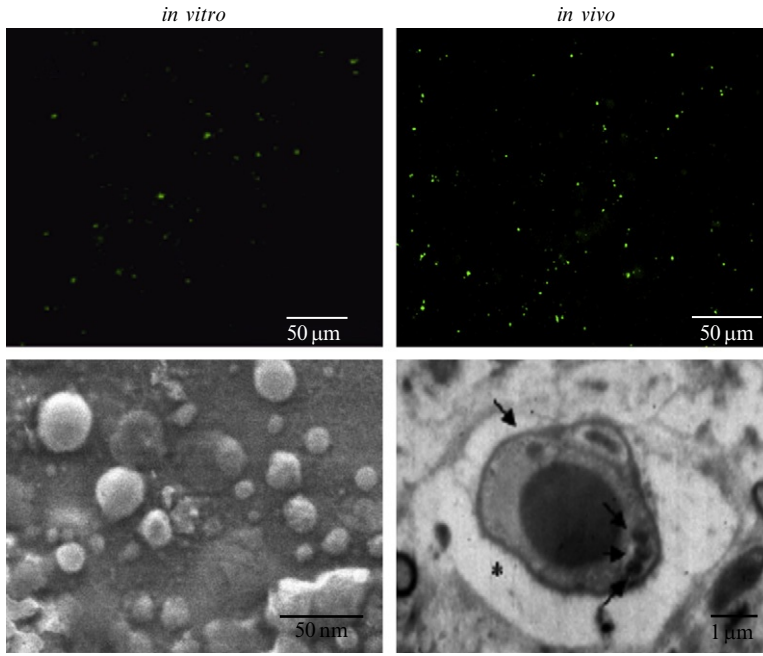

Figure 13.3 Nanoparticles can be visualized by fluorescence microscopy as well as electron microscopy. The column on the left illustrates nanoparticles in aqueous milieu *in vitro*. FITC-labeled nanoparticles are identified as small dots under the fluorescence microscope, and electron dense particles with the electron microscope. After i.v. administration (right column), FITC-labeled nanoparticles are visible in brain tissue sections similar to those observed with *in vitro* imaging. The electron micrograph clearly shows that nanoparticles are transferred into the brain capillary endothelium from circulation (modified from Aktaş *et al.*, 2005, with permission). (For the color version of this figure, the reader is referred to the Web version of this chapter.)

IgG2a is employed to visualize the nanoparticles conjugated with TfRMAb because the TfRMAb is a rat IgG2a. Therefore, the sections are immunostained by using FITC-conjugated goat anti-rat IgG antibody (Sigma, at 1:100 and 1:200 dilutions, in PBS) at room temperature for 60 min to detect TfRMAb-conjugated nanoparticles via the green fluorescence of FITC. Colocalization of the green fluorescence of FITC with the red fluorescence of Nile red ensures that the observed fluorescent dots are nanoparticles (Fig. 13.2). Sections are also coverslipped with mounting medium containing Hoechst 33258 to identify endothelial nuclei. Fluorescence microscopy of these brain sections showed that nanoparticles functionalized with TfRMAb were dispersed within the brain parenchyma, outside the vessel lumens, confirming the successful transfer of nanoparticles across the BBB (Fig. 13.2). Negative controls are carried out by omitting the anti-rat IgG antibody (Karatas *et al.*, 2009).

3.4. Electron microscopy

Nanoparticles can be identified unequivocally by electron microscopy. For this purpose, 1 mm^3 specimens from the frontal cortex, striatum, and the occipital cortices of the hemispheres are examined with transmission electron microscopy. The specimens are fixed in 2.5% gluteraldehyde for 24 h, and after washing in phosphate buffer (pH 7.4), they are fixed in 1% osmium tetroxide (in phosphate buffer) and dehydrated in graded alcohol. After washing the tissues with propylene oxide and embedding them in epoxy-resin embedding media, semithin (2 μm) and ultrathin (60 nm) sections are cut with an LKB-Nova (Bromma, Sweden) ultramicrotome having a glass knife. The sections are stained with methylene blue and examined under a Nikon Optiphot (Japan) light microscope. After trimming, the semi and ultrathin sections are collected on copper grids, stained with uranyl acetate and lead citrate, and examined with a JEOL JEM 1200 EX (Japan) transmission electron microscope. The TfRMAb-conjugated, peptide-unloaded nanoparticles were detected as dense spherical particles with an approximate diameter of 200 nm within the endothelium of the brain blood vessels as well as brain parenchyma (Fig. 13.3; Aktaş *et al.*, 2005).

4. The Neuroprotective Effect of Nanoparticles Loaded with a Caspase Inhibitor

4.1. Focal cerebral ischemia model

Male Swiss albino mice (25–30 g) are housed under diurnal lighting conditions and fasted overnight but allowed *ad libitum* access to water before the experiment. The intraluminal filament middle cerebral artery occlusion (MCAo) model is used to induce focal cerebral ischemia (Gursoy-Ozdemir *et al.*, 2000). In this model, after ligation of the right common and external carotid arteries with a 5-0 silk suture, a nylon filament (8-0) is inserted into the right common carotid artery through a small incision proximal to the bifurcation in anesthetized mice and is advanced up to origin of middle cerebral artery (MCA) via the internal carotid artery (10 mm from the bifurcation) to cause cessation of blood flow in the MCA territory. The tip of filament is coated with silicone resin/hardener mixture (Xantropen M Haereus Kulzer, and Optosil-Xantropen Activator, Bayer) to provide smooth move in the lumen. The filament is withdrawn after 2 h of MCAo to establish reperfusion. Throughout the experiments, the regional cerebral blood flow (rCBF) is monitored by laser Doppler (PF-318 of PeriFlux PF 2B; Perimed) using a fiber optic flexible probe placed over the temporal bone 2 mm posterior, 6 mm lateral to the bregma, and away from large pial vessels. This is instrumental to confirm occlusion and

reperfusion. Physiologic parameters (blood pressure, body temperature, rCBF, pulse rate, and tissue oxygen saturation) are also monitored closely during cerebral ischemia, as described above. There must be no significant differences between the physiologic parameters of the experimental groups, so that the changes determined in infarct volumes could be attributed to the effect of the therapeutics.

4.2. Neuroprotection study groups

To evaluate the neuroprotective effect of nanoparticles loaded with Z-DEVD-FMK, various groups of mice are subjected to 2 h of MCAo and 24 h of reperfusion. Control groups receive either drug unloaded TfRMAb-conjugated nanoparticles or TfRMAb-unconjugated nanoparticles loaded with the peptide. The treatment groups receive injections of TfRMAb-conjugated nanoparticles loaded with 50 ng/mg of Z-DEVD-FMK (low-dose group) or 188 ng/mg of Z-DEVD-FMK (high-dose group). Nanoparticles (1 mg of nanoparticle in 10 μl of saline) are administered just before induction of ischemia via the tail vein in all experimental groups, except in one group of mice that are treated with nanoparticles loaded with a high dose of the caspase inhibitor just before establishing reperfusion (postischemia treatment group; Karatas *et al.*, 2009).

The neuroprotective effect of nanoparticles loaded with the caspase inhibitor can be assessed by neurological evaluation of mice, the infarct volume and caspase activity. Twenty hours after reperfusion, prior to scarification, the neurologic deficit is scored in each animal, with a previously validated scale ranging from 0 to 3; 0 designating no significant neurologic deficit and 3 designating severe neurologic deficit (Huang *et al.*, 1994). Treatment with TfRMAb-conjugated nanoparticles containing Z-DEVD-FMK leads to significant improvement in neurological deficits. The mean ± SEM neurological deficit scores 24 h after reperfusion were 2.8 ± 0.2 in the peptide-free (blank) nanoparticle group, 2.6 ± 0.2 in the TfRMAb-unconjugated nanoparticle group, 2.0 ± 0.2 in the low-dose Z-DEVD-FMK group, 1.5 ± 0.3 in the high-dose Z-DEVD-FMK group, and 2.3 ± 0.2 in the high-dose Z-DEVD-FMK/postischemia group ($p < 0.05$ when compared with the peptide-free (blank) and the TfRMAb-unconjugated group; Karatas *et al.* 2009).

For evaluation of the infarct volume, mice are anesthetized with a lethal dose of chloral hydrate 24 h after reperfusion. Mice are transcardially perfused with 100 ml of heparinized ultra pure water (10 IU/ml) followed by 4% paraformaldehyde and then decapitated. Brains are stored in 4% paraformaldehyde for 48 h, after which 2-mm thick coronal sections are serially cut, starting from the frontal pole. Slices are then embedded in paraffin and 5 μm-thick sections are obtained from the posterior surface of each slab and stained with hematoxylin and eosin. The boundary of the infarct area,

characterized by reduced eosin staining under light microscopy, is outlined using an image analysis software (ImageJ 1.59, NIH, Bethesda, MD) to calculate the infarct volume. We found that the infarct volumes in mice receiving Z-DEVD-FMK-free (blank) and TfRMAb-unconjugated nanoparticles were 43 ± 4 and 50 ± 4 mm^3, respectively (Fig. 13.4). Treatment with nanoparticles loaded with Z-DEVD-FMK significantly and dose-dependently decreased the infarct volume ($p < 0.05$). The volumes were 33 ± 3 mm^3 with low-dose Z-DEVD-FMK, 26 ± 4 mm^3 with high-dose Z-DEVD-FMK and 32 ± 2 mm^3 with high-dose Z-DEVD-FMK, when administered postischemia (Karatas *et al.*, 2009). The neuroprotection obtained in the posttreatment group in which Z-DEVD-FMK was given 2 h after ischemia is of clinical importance, because the therapeutic time window in stroke patients is limited to the first 3 h after stroke onset and the delayed treatment is usually ineffective.

4.3. Determination of caspase-3 activity

Caspase-3 activity in the ischemic brain tissue can also be utilized to assess the effect of systematically administered Z-DEVD-FMK-loaded nanoparticles. Caspases are enzymes of the cysteine–aspartic acid protease family. They are present in cells as zymogens and are activated upon proteolytic cleavage. Assays of caspase-3 activity must take into account several factors, one of which is the efficiency of the active-site histidine and cysteine pair. The histidine imidazole has a pK_a of 6 and cysteine has a pK_a of 8. The optimal caspase-3 activity occurs at pH 7.4 (the intracellular value). It should also be kept in mind that the cysteine side chain must be protonated. For this reason, in all assays, the concentration of active site cysteine is maintained by addition of the reducing agent, dithiothreitol (DTT) at a final concentration of 2 m*M*. Membrane penetration is achieved by the strong hydrophobic reagent 0.1% TX-100, whereas 2 m*M* EGTA, 2 m*M* EDTA, 5 m*M* $MgCl_2$ are added to the buffer composition to keep the intracellular cofactor concentrations constant.

As previous studies showed a peak in caspase-3 activity 1 h after reperfusion (Ma *et al.*, 1998, 2001), mice are sacrificed 2 h after MCAo and 1 h of reperfusion. Brains kept on ice are weighed and homogenized (20%, w/v) using an Omni 5000 homogenizer (Kennisaw, GA) at 3000 rpm in 25 m*M* HEPES, pH 7.4, 2 m*M* EDTA, 2 m*M* EGTA, 2 m*M* DTT, 5 m*M* $MgCl_2$, 0.1% Triton X-100, and 10 μg/ml protease inhibitor mixture. The homogenates are centrifuged at 4 °C, 12,000 × *g* for 20 min. The clear supernatants are used for caspase-3 activity and protein determination. All assays are done at least in duplicate. Caspase-3 activity is determined using the fluorogenic caspase-3 substrate (*N*-acetyl)-Asp-Glu-Val-Asp-7-amino-4-trifluoromethyl-coumarin (Ac-DEVD-AFC) ApoScreen Kit from ICN Biomedicals (Solon, OH). Briefly, 25 μl of tissue homogenate is added to each well in a 96-well

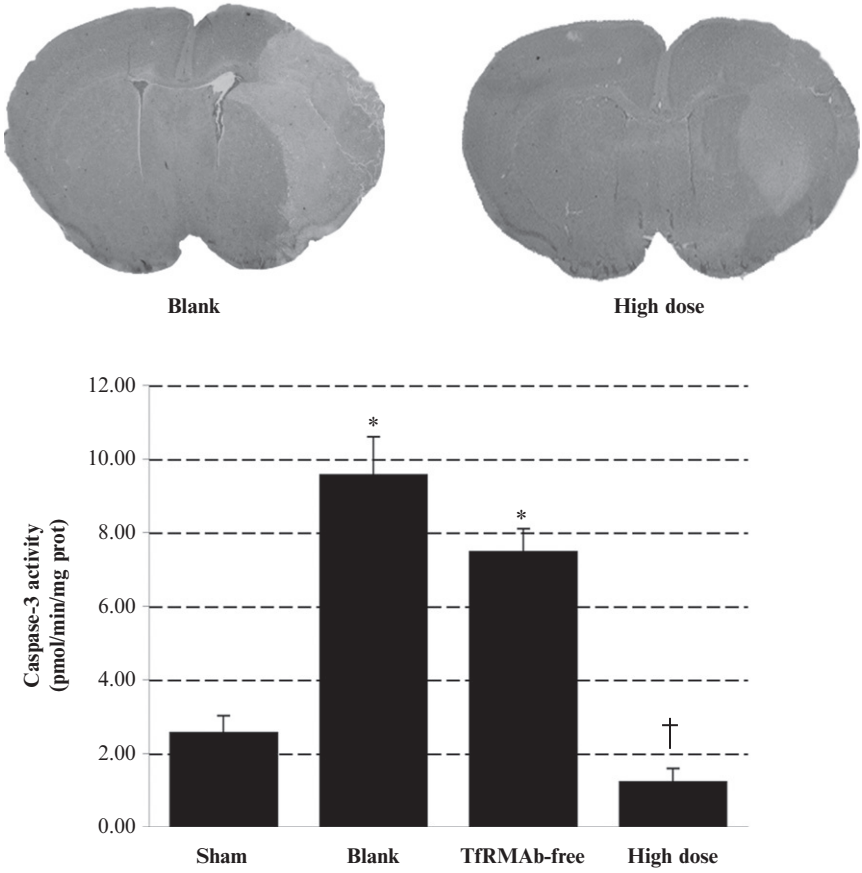

Figure 13.4 Caspase inhibitor-loaded nanoparticles suppress the ischemia-induced increase in caspase-3 activity and provide neuroprotection after systemic administration. Coronal brain sections stained with hematoxylin and eosin illustrate the representative infarct areas (pale) from mice subjected to 2 h of ischemia and 24 h of reperfusion, and treated with blank (control), or high-dose Z-DEVD-FMK-loaded nanoparticles. Caspase-3 activity was detected in hemispheres obtained from mice subjected to either sham surgery or 2 h MCA occlusion and 1 h reperfusion. Nanoparticles loaded with a high dose of Z-DEVD-FMK and conjugated with TfRMAb antibody (high-dose) significantly inhibited caspase-3 activity, whereas nanoparticles not loaded with the peptide (blank) or unconjugated with TfRMAb (TfRMAb-free) were ineffective. *Significant difference when compared with the sham-operated group. †No significant difference when compared with the sham-operated group. Prot, protein (modified from Karatas *et al.*, 2009, with permission). (For the color version of this figure, the reader is referred to the Web version of this chapter.)

plate already containing 222.5 µl of 100 m*M* HEPES, pH 7.4, and 2 m*M* DTT. The reaction is initiated by the addition of fluorogenic 2.5 µl of Ac-DEVD-AFC at a final concentration of 200 µ*M*. Parallel samples are incubated for

25 min with the competitive inhibitor Z-DEVD-FMK (final concentration 40 μM) before adding the substrate. Activity measurements utilizing an end point assay are performed at baseline and 35 min later (excitation 400, emission 505 nm) with a spectrofluorometric plate reader (SpectraMax M2, Molecular Devices, Sunnyvale, CA) and software (SOFTmax Pro 3.1.1, Molecular Devices). Caspase-3 activity (fluorescence units per milligram protein per minute of reaction time) is calculated from the slope of the difference between substrate utilization velocity in the samples with and without caspase-3 inhibitor. This measurement is then converted to picomoles of substrate cleaved per milligram of protein per minute, based on a standard curve for amino-4-trifluoromethylcoumarin. The protein concentration in the supernatant is determined by the Bradford assay. These assays also confirmed the efficient transfer of nanoparticles across the BBB by showing that caspase-3 activity was suppressed significantly in mice receiving conjugated nanoparticles loaded with high-dose Z-DEVD-FMK when compared to mice receiving peptide-free (blank) or TfRMAb-unconjugated nanoparticles ($p < 0.05$; Fig. 13.4; Karatas *et al.*, 2009).

5. Concluding Remarks

Brain-targeted nanoparticles loaded with BBB-impermeable drugs create new and exciting opportunities for treatment of CNS disorders. These nanomedicines not only have the potential of achieving therapeutic drug levels in the brain but may also decrease their systemic side effects by selectively targeting therapeutics to the brain. Although currently used pharmacological end points are useful as screening tools, we need advanced technologies that will allow us to study the *in vivo* kinetics of nanoparticle penetration to the CNS to further develop these novel drug carriers (e.g., by modifying the particle size, shape, and surface characteristics). Moreover, identification of the most efficient carrier (e.g., the insulin receptor) on human brain capillary endothelial cells is necessary to translate these nanotechnologies to the clinic, despite the fact that the mouse TfR system currently provides a satisfactory experimental model.

ACKNOWLEDGMENTS

We wish to thank all of our colleagues including our collaborators in France (Patrick Couvreur, Karine Andrieux from Universite´ Paris Sud) and Spain (Eduardo Fernandez-Megia, Ramon Novoa-Carballal, Ricardo Riguera from Universidad de Santiago de Compostela) for their important contributions to the development of the nanoparticles used in studies cited in the chapter. Dr. Turgay Dalkara's work is supported by the Turkish Academy of Sciences.

REFERENCES

Abbott, N. J., Rönnbäck, L., and Hansson, E. (2006). Astrocyte-endothelial interactions at the blood-brain barrier. *Nat. Rev. Neurosci.* **7,** 41–53.

Aktaş, Y., Yemisci, M., Andrieux, K., Gürsoy, R. N., Alonso, M. J., Fernandez-Megia, E., Novoa-Carballal, R., Quiñoá, E., Riguera, R., Sargon, M. F., Celik, H. H., Demir, A. S., *et al.* (2005). Development and brain delivery of chitosan-PEG nanoparticles functionalized with the monoclonal antibody OX26. *Bioconjug. Chem.* **16,** 1503–1511.

Begly, D. M. (1996). The blood-brain-barrier: Principles for targeting peptides and drugs to the central nervous system. *J. Pharm. Pharmacol.* **48,** 136–146.

Brigger, I., Morizet, J., Aubert, G., Chacun, H., Terrier-Lacombe, M. J., Couvreur, P., and Vassal, G. (2002). Poly(ethylene glycol)-coated hexadecylcyanoacrylate nanoparticles display a combined effect for brain tumor targeting. *J. Pharmacol. Exp. Ther.* **303,** 928–936.

Chen, J., Nagayama, T., Jin, K., Stetler, R. A., Zhu, R. L., Graham, S. H., and Simon, R. P. (1998). Induction of caspase-3-like protease may mediate delayed neuronal death in the hippocampus after transient cerebral ischemia. *J. Neurosci.* **18,** 4914–4928.

Fernandez-Megia, E., Novoa-Carballal, R., Quinoa, E., and Riguera, R. (2007). Conjugation of bioactive ligands to PEG-grafted chitosan at the distal end of PEG. *Biomacromolecules* **8,** 833–842.

Gessner, A., Olbrich, C., Schröder, W., Kayser, O., and Müller, R. H. (2001). The role of plasma proteins in brain targeting: Species dependent protein adsorption patterns on brain-specific lipid drug conjugate (LDC) nanoparticles. *Int. J. Pharm.* **214,** 87–91.

Gursoy-Ozdemir, Y., Bolay, H., Saribas, O., and Dalkara, T. (2000). Role of endothelial nitric oxide generation and peroxynitrite formation in reperfusion injury after focal cerebral ischemia. *Stroke* **31,** 1974–1981.

Hara, H., Friedlander, R. M., Gagliardini, V., Ayata, C., Fink, K., Huang, Z., Shimizu-Sasamata, M., Yuan, J., and Moskowitz, M. A. (1997). Inhibition of interleukin 1beta converting enzyme family proteases reduces ischemic and excitotoxic neuronal damage. *Proc. Natl. Acad. Sci. USA* **94,** 2007–2012.

Huang, Z., Huang, P. L., Panahian, N., Dalkara, T., Fishman, M. C., and Moskowitz, M. A. (1994). Effects of cerebral ischemia in mice deficient in neuronal nitric oxide synthase. *Science* **265,** 1883–1885.

Jefferies, W. A., Brandon, M. R., Hunt, S. V., Williams, A. F., Gatter, K. C., and Mason, D. Y. (1984). Transferrin receptor on endothelium of brain capillaries. *Nature* **312,** 162–163.

Karatas, H., Aktaş, Y., Gursoy-Ozdemir, Y., Bodur, E., Yemisci, M., Caban, S., Vural, A., Pinarbasli, O., Capan, Y., Fernandez-Megia, E., Novoa-Carballal, R., Riguera, R., *et al.* (2009). A nanomedicine transports a peptide caspase-3 inhibitor across the blood-brain barrier and provides neuroprotection. *J. Neurosci.* **29,** 13761–13769.

Kreuter, J. (2001). Nanoparticulate systems for brain delivery of drugs. *Adv. Drug Deliv. Rev.* **47,** 65–81.

Lee, H. J., Engelhardt, B., Lesley, J., Bickel, U., and Pardridge, W. M. (2000). Targeting rat anti-mouse transferrin receptor monoclonal antibodies through bloodbrain barrier in mouse. *J. Pharmacol. Exp. Ther.* **292,** 1048–1052.

Ma, J., Endres, M., and Moskowitz, M. A. (1998). Synergistic effects of caspase inhibitors and MK-801 in brain injury after transient focal cerebral ischaemia in mice. *Br. J. Pharmacol.* **124,** 756–762.

Ma, J., Qiu, J., Hirt, L., Dalkara, T., and Moskowitz, M. A. (2001). Synergistic protective effect of caspase inhibitors and bFGF against brain injury induced by transient focal ischaemia. *Br. J. Pharmacol.* **133,** 345–350.

Namura, S., Zhu, J., Fink, K., Endres, M., Srinivasan, A., Tomaselli, K. J., Yuan, J., and Moskowitz, M. A. (1998). Activation and cleavage of caspase-3 in apoptosis induced by experimental cerebral ischemia. *J. Neurosci.* **18,** 3659–3668.

Pardridge, W. M. (2007). Drug targeting to the brain. *Pharm. Res.* **24,** 1733–1744.

Pardridge, W. M., Buciak, J. L., and Friden, P. M. (1991). Selective transport of an anti transferrin receptor antibody through the blood-brain barrier *in vivo*. *J. Pharmacol. Exp. Ther.* **259,** 66–70.

Royer, G. P., and Anantharmaiah, G. (1979). Peptide synthesis in water and the use of immobilized carboxypeptidase Y for deprotection. *J. Am. Chem. Soc.* **101,** 3394–3396.

Schielke, G. P., Yang, G. Y., Shivers, B. D., and Betz, A. L. (1998). Reduced ischemic brain injury in interleukin-1 beta converting enzyme-deficient mice. *J. Cereb. Blood Flow Metab.* **18,** 180–185.

Zensi, A., Begley, D., Pontikis, C., Legros, C., Mihoreanu, L., Wagner, S., Büchel, C., von Briesen, H., and Kreuter, J. (2009). Albumin nanoparticles targeted with Apo E enter the CNS by transcytosis and are delivered to neurones. *J. Control. Release* **137,** 78–86.